

Interaction Notes

Note 297

27 July 1976

Transient Response of a Helical Antenna

by

Bharadwaja K. Singaraju
Air Force Weapons Laboratory*

and

Robert L. Gardner
Air Force Weapons Laboratory**

DEPARTMENT OF THE AIR FORCE
AFRL/DE 0-PA

OCT 20 2000

CLEARED THIS INFORMATION
FOR PUBLIC RELEASE

Abstract

In this report, two integral equation representations for a helical antenna are derived. Analytical expressions for the natural frequencies and natural modes are calculated using Hallén type integral equation for a loosely wound helix, while an integral equation of Pocklington type is used to calculate these numerically for a helix of arbitrary pitch angle. Trajectories of the natural frequencies of the helix are plotted as the pitch angle is changed. Using the natural frequencies and natural modes, transient response of the helix is calculated for three different incident pulses, and comparisons are made with measured values.

* Now at Dikewood Industries, Inc., Albuquerque, New Mexico.

** Now at the Department of Physics, University of Colorado, Boulder, Colorado.

AFRL/DE 20-475

PREFACE

The authors wish to thank Drs. Carl E. Baum, James L. Gilbert, and Kelvin S.H. Lee for many discussions on this subject.

I. Introduction

Helical antennas are used in satellite communication systems because of their narrow beam width. Because of extensive use of helical antennas in satellite structures, a systematic development of transient response of this type of antenna to an incident field is necessary. In this work the natural frequencies and natural modes of a helical antenna are found.

The transient response of such an antenna is obtained by using Singularity Expansion Method (SEM).¹

II. Hallén Type Integral Equation for a Helical Antenna

Analytical calculations of natural frequencies, natural modes and induced currents of wire antennas are easy to perform in the Hallén integral equation formulation. If a thin wire of radius a is bent into an arbitrary shape, if the radius is small compared to the length, the Hallén integral equation can be written as²

$$\int_0^{\ell} \tilde{K}(\xi, \xi') \tilde{I}(\xi') d\xi' - \cosh\left(\frac{s}{c} \xi\right) \int_0^{\ell} \tilde{G}(0, \xi') \tilde{I}(\xi') (\hat{\mathbf{i}}_{\xi_0} \cdot \hat{\mathbf{i}}_{\xi}) d\xi'$$

$$= A \sinh\left(\frac{s}{c} \xi\right) - \frac{1}{Z_0} \int_0^{\ell} \hat{\mathbf{i}}_{\xi} \cdot \tilde{\mathbf{E}}_{\text{inc}}(\xi') \sinh\left\{\frac{s}{c}(\xi - \xi')\right\} d\xi' \quad (2.1)$$

where the superscript \sim (tilde) denotes bilateral Laplace transformed quantities, $\hat{\mathbf{i}}_{\xi}$ is the unit vector tangential to the wire at ξ while $\hat{\mathbf{i}}_{\xi_0}$ is the unit tangent vector to the wire at $\xi = 0$, ℓ the length of the wire, s the complex radian frequency, c the speed of light in free space, Z_0 the free space impedance and

$$\tilde{K}(\xi, \xi') = \tilde{G}(\xi, \xi') (\hat{\mathbf{i}}_{\xi} \cdot \hat{\mathbf{i}}_{\xi'}) - \int_0^{\xi} \left[\frac{\partial \tilde{G}(\eta, \xi')}{\partial \eta} (\hat{\mathbf{i}}_{\eta} \cdot \hat{\mathbf{i}}_{\xi'}) \right.$$

$$\left. + \frac{\partial \tilde{G}(\eta, \xi)}{\partial \xi'} + \tilde{G}(\eta, \xi') \frac{\partial (\hat{\mathbf{i}}_{\eta} \cdot \hat{\mathbf{i}}_{\xi'})}{\partial \eta} \right] \cosh \frac{s}{c} (\xi - \eta) d\eta \quad (2.2)$$

with the free space Green's function given by

$$\tilde{G}(\xi, \xi') = \frac{e^{-\frac{sR}{c}}}{4\pi R} = \frac{e^{-\gamma R}}{4\pi R} \quad (2.3)$$

with

$$R = |\vec{r} - \vec{r}'| \quad (2.4)$$

$$\gamma = \frac{\underline{S}}{c} = \text{complex propagation constant} \quad (2.5)$$

In equation 2.1 the end condition $\tilde{I}(0)=0$ is automatically satisfied. If the wire is bent into a helix as shown in figure 1, then

$$\begin{aligned} \vec{r} - \vec{r}' = & \rho_0 (\cos(\phi) - \cos(\phi')) \hat{i}_x + \rho_0 (\sin(\phi) - \sin(\phi')) \hat{i}_y \\ & + \{ \rho_0 \tan(\alpha) (\phi - \phi') - a (\sin(\theta) - \sin(\theta')) \} \hat{i}_z \end{aligned} \quad (2.6)$$

where ρ_0 is the radius of the helix and α the pitch angle. If we then ignore the θ dependence, i.e., assume the current to be uniform around the wire, and if we assume that the wire radius is small compared to the radius of the helix, equation 2.6 can be rewritten as

$$|\vec{r} - \vec{r}'| \approx \rho_0 \left[4 \sin^2 \left(\frac{\phi - \phi'}{2} \right) + \tan^2(\alpha) (\phi - \phi')^2 + \frac{a^2}{\rho_0^2} \right]^{\frac{1}{2}} \quad (2.7)$$

Notice that in equation 2.7 the distance is a function of $|\phi - \phi'|$ and α^2 while in equation 2.6 it is a more complicated function of ϕ and ϕ' . This type of dependence, i.e., equation 2.7, makes the integration kernel to be a closed type. As such, in the moments method formulation, if proper expansion functions are used, the impedance matrix becomes Toplitz symmetric.

Using equation 2.1 and 2.7, the integral equation for a helix can be written as

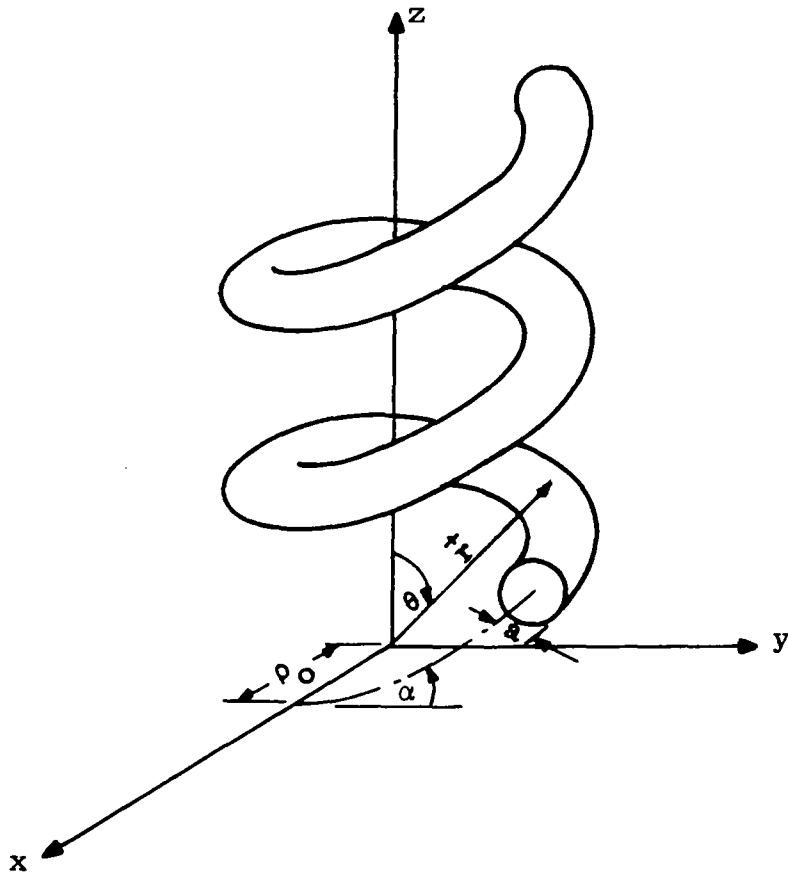


Figure 1. Helix of Finite Wire Radius

$$\int_0^{\phi_u} \tilde{K}(\phi-\phi') \tilde{I}(\phi') d\phi'$$

$$-\cos^2(\alpha) \cosh \left\{ \frac{S}{c} \rho_0 \sec(\alpha) \phi \right\} \int_0^{\phi_u} \tilde{G}(\phi') \tilde{I}(\phi') [\cos(\phi') + \tan^2(\alpha)] d\phi'$$

$$= A \sinh \left\{ \frac{S}{c} \rho_0 \sec(\alpha) \phi \right\} + \frac{4\pi\rho_0}{Z_0} \int_0^{\phi_u} \hat{t}_\xi \cdot \tilde{\mathbf{E}}_{\text{inc}}(\xi') \sinh \left\{ \frac{S}{c} \rho_0 \sec(\alpha) (\phi-\phi') \right\} d\phi'$$

with

(2.8)

$$\tilde{K}(\phi-\phi') = \tilde{G}(\phi, \phi') [\cos^2(\alpha) \cos(\phi-\phi') + \sin^2(\alpha)]$$

$$- \cos^3(\alpha) \int_0^\phi \left[\frac{d}{d\phi_\eta} \{ \cos(\phi_\eta - \phi') \tilde{G}(\phi_\eta, \phi') \} + \right.$$

$$\left. \{ 2 \sec^2(\alpha) - 1 \} \frac{d\tilde{G}(\phi_\eta, \phi')}{d\phi_\eta} \right] \cosh \left\{ \frac{S}{c} \rho_0 \sec(\alpha) (\phi_\eta - \phi') \right\} d\phi_\eta \quad (2.9)$$

where ϕ_u is equal to number of turns times 2π radians and

$$\tilde{G}(\phi, \phi') = \frac{e^{-\gamma \rho_0 \left\{ 4 \sin^2 \left(\frac{\phi-\phi'}{2} \right) + \tan^2(\alpha) (\phi-\phi')^2 + \frac{a^2}{2} \right\}^{\frac{1}{2}}}}{\rho_0 \left\{ 4 \sin^2 \left(\frac{\phi-\phi'}{2} \right) + \tan^2(\alpha) (\phi-\phi')^2 + \frac{a^2}{2} \right\}^{\frac{1}{2}}} \quad (2.10)$$

If we set $\alpha = \pi/2$ in equations 2.8, 2.9 and 2.10 while keeping the total length of the wire constant, we obtain the integral equation for a straight thin wire while setting $\alpha = 0$ yields the equation for an open ended arc antenna. If the pitch angle α is large, i.e., a loosely wound helix, it can be shown that the integral in equation 2.9 can be ignored yielding

$$\tilde{K}(\phi-\phi') \approx \tilde{G}(\phi, \phi') [\cos^2(\alpha) \cos(\phi-\phi') + \sin^2(\alpha)] \quad (2.11)$$

considerably simplifying equation 2.9.

III. Analytical Calculations of the Natural Frequencies and Natural Modes

Natural frequencies are the complex frequencies s_n where the response has pole while natural modes (left or right) are the solutions of the homogeneous equation. Considering the case where the pitch angle is large, we can write equation 2.8 as

$$\int_0^{\phi_u} \tilde{I}(\phi') \tilde{G}(\phi, \phi') [\cos^2(\alpha) \cos(\phi - \phi') + \sin^2(\alpha)] d\phi' - \cosh \left\{ \frac{s}{c} \rho_0 \sec(\alpha) \phi \right\} \int_0^{\phi_u} \tilde{G}(\phi') \tilde{I}(\phi') [\cos^2(\alpha) \cos(\phi') + \sin^2(\alpha)] d\phi' \quad (3.1)$$

$$= A \sinh \left\{ \frac{s}{c} \rho_0 \sec(\alpha) \phi \right\} + \frac{4\pi\rho_0}{Z_0} \int_0^{\phi} \tilde{I}_{\xi} \cdot \tilde{E}_{inc}(\xi') \sinh \left\{ \frac{s}{c} \rho_0 \sec(\alpha) (\phi - \phi') \right\} d\phi'$$

while

$$\tilde{G}(\phi, \phi') \approx \frac{e^{-\frac{s}{c} \rho_0 \sec(\alpha) \left\{ (\phi - \phi')^2 + \frac{a^2}{2} \cos^2(\alpha) \right\}^{\frac{1}{2}}}}{\left\{ (\phi - \phi')^2 + \frac{a^2}{2} \cos^2(\alpha) \right\}^{\frac{1}{2}}} \quad (3.2)$$

Equation 3.1 can be considered to contain the correction terms for a loop and a straight wire. Since a helix is neither a straight wire nor a loop, it is logical to expect this integral equation to contain terms corresponding to both the straight wire and a loop.

Considering the first integral in equation 3.1, denoting it by $\tilde{f}(\phi)$

$$\tilde{f}(\phi) \equiv \int_0^{\phi_u} \tilde{I}(\phi') e^{-\frac{s}{c} \rho_0 \sec(\alpha) \left\{ (\phi - \phi')^2 + \frac{a^2}{2} \cos^2(\alpha) \right\}^{\frac{1}{2}}} [\cos^2(\alpha) \cos(\phi') + \sin^2(\alpha)] d\phi' \equiv \tilde{f}_1(\phi) + \tilde{f}_2(\phi) \quad (3.3)$$

where

$$\tilde{f}_1(\phi) \equiv \cos^2(\alpha) \int_0^{\phi_u} \tilde{I}(\phi') \cos(\phi - \phi') \frac{e^{-\frac{s}{c} \rho_0 \sec(\alpha) \{(\phi - \phi')^2 + \frac{a^2}{2} \cos^2(\alpha)\}^{\frac{1}{2}}}}{\{(\phi - \phi')^2 + \frac{a^2}{2} \cos^2(\alpha)\}^{\frac{1}{2}}} d\phi' \quad (3.4)$$

$$\tilde{f}_2(\phi) \equiv \sin^2(\alpha) \int_0^{\phi_u} \tilde{I}(\phi') \frac{e^{-\frac{s}{c} \rho_0 \sec(\alpha) \{(\phi - \phi')^2 + \frac{a^2}{2} \cos^2(\alpha)\}^{\frac{1}{2}}}}{\{(\phi - \phi')^2 + \frac{a^2}{2} \cos^2(\alpha)\}^{\frac{1}{2}}} d\phi' \quad (3.5)$$

Since the radius of the wire is very small compared to the radius of the helix, we can write equations 3.4 and 3.5 as a sum of two integrals, one a function of a while the other independent of a , as^{3,4}

$$\tilde{f}_1(\phi) \approx \cos^2(\alpha) \left[\tilde{I}(\phi) \int_0^{\phi_u} \frac{\cos(\phi - \phi')}{\{(\phi - \phi')^2 + \frac{a^2}{2} \cos^2(\alpha)\}^{\frac{1}{2}}} d\phi' + \int_0^{\phi_u} \cos(\phi - \phi') \frac{\tilde{I}(\phi') e^{-\frac{s}{c} \rho_0 \sec(\alpha) |\phi - \phi'|}}{|\phi - \phi'|} - \tilde{I}(\phi) d\phi' \right] \quad (3.6)$$

while

$$\tilde{f}_2(\phi) \approx \sin^2(\alpha) \left[\tilde{I}(\phi) \int_0^{\phi_u} \frac{1}{\{(\phi - \phi')^2 + \frac{a^2}{2} \cos^2(\alpha)\}^{\frac{1}{2}}} d\phi' + \int_0^{\phi_u} \frac{\tilde{I}(\phi') e^{-\frac{s}{c} \rho_0 \sec(\alpha) |\phi - \phi'|}}{|\phi - \phi'|} - \tilde{I}(\phi) d\phi' \right] \quad (3.7)$$

We now define the fatness factor Ω as

$$\Omega = 2\ell n \left(\frac{\rho_0 \sec(\alpha) \phi_u}{a} \right) \equiv 2\ell n \left(\frac{\ell}{a} \right) \quad (3.8)$$

where ℓ is the total length of the wire with which the helix is constructed. This definition is consistent with the definition of the fatness factor⁵ for linear antennas. Using equation 3.8, we can evaluate equation 3.6 as⁶

$$\begin{aligned} \tilde{f}_1(\phi) &= \cos^2(\alpha) \{ \Omega + 2\ell n(2) - 2\zeta + \text{Ci}(\phi) + \text{Ci}(\phi_u - \phi) \} \tilde{I}(\phi) \\ &+ \int_0^{\phi_u} \cos(\phi - \phi') \frac{\tilde{I}(\phi') e^{-\frac{s}{c} \rho_0 \sec(\alpha) |\phi - \phi'|} - \tilde{I}(\phi)}{|\phi - \phi'|} d\phi' \end{aligned} \quad (3.9)$$

where $\text{Ci}(\phi)$ is the cosine integral while ζ is the Euler's constant.

$$\begin{aligned} \tilde{f}_2(\phi) &= \sin^2(\alpha) \tilde{I}(\phi) \left\{ \Omega + \ell n \left\{ \frac{4(\phi_u - \phi)}{\phi_u^2} \phi \right\} \right\} \\ &+ \int_0^{\phi_u} \frac{\tilde{I}(\phi') e^{-\frac{s}{c} \rho_0 \sec(\alpha) |\phi - \phi'|} - \tilde{I}(\phi)}{|\phi - \phi'|} d\phi' \end{aligned} \quad (3.10)$$

As a consequence of equations 3.9 and 3.10, the equation for the current on the helix can be written as

$$\begin{aligned}
& \tilde{I}(\phi) + \frac{1}{\Omega} \left[\sin^2(\alpha) \ln \left\{ \frac{4(\phi_u - \phi)\phi}{\phi_u^2} \right\} \tilde{I}(\phi) \right. \\
& + \cos^2(\alpha) \{2 \ln(2) - 2\zeta + \text{Ci}(\phi) + \text{Ci}(\phi_u - \phi)\} \tilde{I}(\phi) \\
& + \int_0^{\phi_u} \left[\frac{-\frac{S}{c} \rho_0 \sec(\alpha) |\phi - \phi'|}{\left\{ \frac{\tilde{I}(\phi') e^{-\frac{S}{c} \rho_0 \sec(\alpha) |\phi - \phi'|}}{|\phi - \phi'|} - \tilde{I}(\phi) \right\}} \right. \\
& \left. \left. \left\{ \sin^2(\alpha) + \cos^2(\alpha) \cos(\phi - \phi') \right\} \right] d\phi' \right. \\
& \left. - \cosh \left\{ \frac{S}{c} \rho_0 \sec(\alpha) \phi \right\} \int_0^{\phi_u} \tilde{I}(\phi') \frac{e^{-\frac{S}{c} \rho_0 \sec(\alpha) \left\{ \phi'^2 + \frac{a^2}{2} \sec^2(\alpha) \right\}^{\frac{1}{2}}}}{\left\{ \phi'^2 + \frac{a^2}{2} \sec^2(\alpha) \right\}^{\frac{1}{2}}} \right. \\
& \left. \left. \left\{ \sin^2(\alpha) + \cos^2(\alpha) \cos(\phi - \phi') \right\} d\phi' \right] \right. \\
& = A_1 \sinh \left\{ \frac{S}{c} \rho_0 \sec(\alpha) \phi \right\} + \frac{4\pi\rho_0}{\Omega Z_0} \int_0^{\phi} \hat{I}_{\xi} \cdot \tilde{\mathbf{E}}_{\text{inc}}(\xi') \\
& \sinh \left\{ \frac{S}{c} \rho_0 \sec(\alpha) (\phi - \phi') \right\} d\phi' \tag{3.11}
\end{aligned}$$

If we impose the end condition $\tilde{I}(\phi_u) = 0$ in equation 3.11, we obtain

$$\begin{aligned}
& \int_0^{\phi_u} \left[\tilde{I}(\phi') \frac{e^{-\frac{s}{c} \rho_0 \sec(\alpha) |\phi_u - \phi'|}}{|\phi_u - \phi'|} \{\sin^2(\alpha) + \cos^2(\alpha) \cos(\phi_u - \phi')\} \right] d\phi' \\
& - \cosh \left\{ \frac{s}{c} \rho_0 \sec(\alpha) \phi_u \right\} \int_0^{\phi_u} \tilde{I}(\phi') \frac{e^{-\frac{s}{c} \rho_0 \sec(\alpha) \left\{ \phi'^2 + \frac{a^2}{2} \sec^2(\alpha) \right\}^{\frac{1}{2}}}}{\left\{ \phi'^2 + \frac{a^2}{2} \sec^2(\alpha) \right\}^{\frac{1}{2}}} \\
& \{\sin^2(\alpha) + \cos^2(\alpha) \cos(\phi_u - \phi')\} d\phi'
\end{aligned}$$

$$= A_1 \sinh \left\{ \frac{s}{c} \rho_0 \sec(\alpha) \phi_u \right\} + \frac{4\pi \rho_0}{\Omega Z_0} \int_0^{\phi_u} \tilde{I}_\xi \cdot \tilde{E}_{inc}(\xi')$$

$$\sinh \left\{ \frac{s}{c} \rho_0 \sec(\alpha) (\phi_u - \phi') \right\} d\phi' \tag{3.12}$$

It is possible to eliminate the unknown constant A_1 between equations 3.11 and 3.12. If the induced current $I(\phi)$ is of interest, this is a necessity.

In order to obtain the natural frequencies, we set the incident field to be zero in equation 3.12 thus obtaining

$$\begin{aligned}
A_1 \sinh \left\{ \frac{s}{c} \rho_0 \sec(\alpha) \phi_u \right\} &= \frac{1}{\Omega} \int_0^{\phi_u} \tilde{I}(\phi') \frac{e^{-\frac{s}{c} \rho_0 \sec(\alpha) |\phi_u - \phi'|}}{|\phi_u - \phi'|} \\
& \{\sin^2(\alpha) + \cos^2(\alpha) \cos(\phi_u - \phi')\} d\phi' \\
- \cosh \left\{ \frac{s}{c} \rho_0 \sec(\alpha) \phi_u \right\} & \int_0^{\phi_u} \tilde{I}(\phi') \frac{e^{-\frac{s}{c} \rho_0 \sec(\alpha) \left\{ \phi'^2 + \frac{a^2}{2} \sec^2(\alpha) \right\}^{\frac{1}{2}}}}{\left\{ \phi'^2 + \frac{a^2}{2} \sec^2(\alpha) \right\}^{\frac{1}{2}}} \\
& \{\sin^2(\alpha) + \cos^2(\alpha) \cos(\phi_u - \phi')\} d\phi'
\end{aligned} \tag{3.13}$$

Setting $\tilde{I}_n = A_1 \sin\{\frac{n\pi}{l} \rho_0 \sec(\alpha)\phi\}$ in equation 3.13 and expanding in terms of $1/\Omega$, if we neglect terms of order $1/\Omega^2$, after considerable algebraic manipulations we obtain the natural frequencies s_n to be

$$s_n \approx \frac{n\pi c}{l} \left[i - \frac{1}{\Omega} \sin^2(\alpha) \frac{E(2n\pi)}{n\pi} - \frac{1}{\Omega} \frac{\cos^2(\alpha)}{2} \right\} - \frac{2}{n\pi} \{ \zeta + \ell n(\phi_u) - \text{Ci}(\phi_u) \} + \frac{E(2n\pi - \phi_u)}{n\pi} + \frac{E(2n\pi + \phi_u)}{n\pi} \left. \right] \quad n = +1, 2, \dots \quad (3.14)$$

where $E(x)$ is the exponential integral, $\text{Ci}(x)$ the cosine integral.

As should be expected, if we set $\alpha = \pi/2$ in equation 3.14 we obtain the natural frequencies of a straight thin wire. It is interesting to note that in equation 3.14 terms associated with $\sin^2(\alpha)$ are the correction terms of a straight thin wire, while $\cos^2(\alpha)$ terms are those that are associated with the correction terms of an openended loop. Hence a helix can be looked at as a combination of a straight wire along with a multi-turn loop. Using the natural frequencies given by equation 3.14, the natural modes $\tilde{I}_n(\phi)$ can be calculated to be

$$\begin{aligned}
\tilde{I}_n(\phi) \approx & \sin\left\{\frac{n\pi}{\ell} \rho_0 \sec(\alpha)\phi\right\} + \frac{\sin^2(\alpha)}{\Omega} \left[-\ell n \left\{ \frac{4(\phi_u - \phi)\phi}{\phi_u^2} \right\} \sin\left(\frac{n\pi}{\ell} \rho_0 \sec(\alpha)\phi\right) \right. \\
& + i \cos\left(\frac{n\pi}{\ell} \rho_0 \sec(\alpha)\phi\right) \left\{ \frac{2\rho_0 \sec(\alpha)\phi - \ell}{\ell} \right\} E(2n\pi) \\
& + \frac{i}{2} \left[e^{-i\frac{n\pi}{\ell} \rho_0 \sec(\alpha)\phi} E\left(2n\pi \frac{\phi_u - \phi}{\phi_u}\right) - e^{i\frac{n\pi}{\ell} \rho_0 \sec(\alpha)\phi} E\left(2n\pi \frac{\phi}{\phi_u}\right) \right] \\
& + \frac{\cos^2(\alpha)}{\Omega} \left[i\{-2\{\zeta + \ell n(\phi_u)\} - \text{Ci}(\phi_u)\} + E(2n\pi - \phi_u) \right. \\
& + E(2n\pi + \phi_u) \left. \right] \left\{ \frac{\rho_0 \sec(\alpha)\phi}{\ell} \right\} \cos\left\{\frac{n\pi}{\ell} \rho_0 \sec(\alpha)\phi\right\} \\
& - \{2\ell n(2) - 2\zeta + \text{Ci}(\phi) + \text{Ci}(\phi_u - \phi)\} \sin\left\{\frac{n\pi}{\ell} \rho_0 \sec(\alpha)\phi\right\} \\
& - \frac{i}{4} \cos\left(\frac{n\pi}{\ell} \rho_0 \sec(\alpha)\phi\right) \{2\zeta + 2\ell n(\phi_u) - \text{Ci}(\phi_u) + E(2n\pi - \phi_u) + E(2n\pi + \phi_u)\} \\
& + O(1/\Omega^2)
\end{aligned} \tag{3.15}$$

As can be seen from equation 3.15, the natural modes of a helix contain terms which are associated with the straight wire and those that are associated with an open ended loop. From equation 3.14, even for a loosely wound helix, estimating the natural frequencies from the total length of the wire is a very crude approximation. If the helix is tightly wound, the integral in equation 2.3 can no longer be neglected. Inclusion of this integral in analytical calculations will be too complicated and hence will not be treated here.

IV. Numerical Evaluation of the Natural Frequencies and Natural Modes

The Hallén type integral equation derived previously can be used to calculate the natural frequencies and natural modes of a helical antenna numerically. However, because of the double integration involved in equation 2.8, this representation is not used for numerical computational purposes. Pocklington form of integro-differential equation for an arbitrarily bent thin wire is given by⁷

$$\int_{-L}^L \left[\frac{\partial^2}{\partial \xi \partial \xi'} \tilde{G}(\xi, \xi') + \frac{s^2}{c^2} \tilde{G}(\xi, \xi') \right] \tilde{I}(\xi') d\xi' = s \epsilon_0 \hat{I}_{\xi} \cdot \tilde{E}_{inc}(\xi) \quad (4.1)$$

where $\tilde{G}(\xi, \xi')$ is the free space Green's function. If the wire is bent into a helix and if we assume that it is over a ground plane, the integro-differential equation for this case can be written as

$$\int_{-\phi_u}^{\phi_u} \left[\frac{\partial^2 \tilde{G}(\phi, \phi')}{\partial \phi \partial \phi'} + \frac{s^2}{c^2} \rho_0 \sec^2(\alpha) \{ \cos^2(\alpha) \cos(\phi - \phi') + \sin^2(\alpha) \} \tilde{G}(\phi, \phi') \right] \tilde{I}(\phi') d\phi' = s \epsilon_0 \hat{I}_{\xi} \cdot \tilde{E}_{inc}(\xi) \quad (4.2)$$

where

$$\tilde{G}(\phi, \phi') = \frac{e^{-j \sqrt{\frac{s^2}{c^2} \rho_0 \sec^2(\alpha) [4 \cos^2(\alpha) \sin^2(\frac{\phi - \phi'}{2}) + \sin^2(\alpha) (\phi - \phi')^2 + \frac{a^2}{\rho_0^2 \sec^2(\alpha)}]}]}{4 \pi \rho_0 \sec(\alpha) [4 \cos^2(\alpha) \sin^2(\frac{\phi - \phi'}{2}) + \sin^2(\alpha) (\phi - \phi')^2 + \frac{a^2}{\rho_0^2 \sec^2(\alpha)}]^{\frac{1}{2}}} \quad (4.3)$$

and ϕ_u is equal to the number of turns of the helix times 2π . Green's function of the form given by equation 4.3 makes the kernel a closed type kernel. After considerable algebraic manipulations, equation 4.2 can be rewritten by the help of equation 4.3 as

$$\int_{-\phi_u}^{\phi_u} e^{-\gamma r} \left[\frac{(\underline{1} + \gamma r)(2r^2 - 3a^2) + \gamma^2 r^2 \{ \cos^2(\alpha)(1 - \cos(\phi - \phi')) - a^2 [1 - \cos^2(\alpha) 1 - \cos(\phi - \phi')] \}}{r^5} \right]$$

$$\rho_o \sec(\alpha) \tilde{I}(\phi') d\phi' = -4\pi s \epsilon_o \tilde{I}_\xi \cdot \tilde{E}_{inc}(\xi) \quad (4.4)$$

where

$$r = \rho_o \sec(\alpha) \left[4 \cos^2(\alpha) \sin^2\left(\frac{\phi - \phi'}{2}\right) + \sin^2(\alpha)(\phi - \phi')^2 \frac{a^2}{\rho_o^2 \sec^2(\alpha)} \right]^{\frac{1}{2}} \quad (4.5)$$

If we set $\alpha = \pi/2$ in equations 4.4 and 4.5 by keeping $\pm \rho_o \sec(\alpha) \phi_u$ constant, we obtain Richmond's expression for a straight thin wire.⁷

In moments method formulation⁸ (MoM), equation 4.4 can be written as

$$(\tilde{Z}_{m,n}) \cdot (\tilde{I}_n) = (\tilde{V}_m) \quad (4.6)$$

Natural frequencies s_n are those points in the complex s plane where the determinant of the matrix $(\tilde{Z}_{m,n})$ is zero while the natural modes are the solutions of the homogeneous equation at $s = s_n$.

In table 1, the first layer natural frequencies of a helix which has 8 turns, is over a perfectly conducting infinite ground plane, has radius $\rho_o = 5.5$ cm, wire radius $a = .635$ cm and pitch angle $\alpha = 9.64^\circ$ are shown. These natural frequencies have been calculated using the computer program SEARCH⁹, and the normalized natural frequency s'_n is given by

$$s'_n = \frac{s_n \ell}{\pi c} \quad (4.7)$$

where ℓ is the total length of the wire used in the helix and its image (≈ 5.6 m), while c is the speed of light in free space ($c \approx 3 \times 10^8$ m/s).

n	LAYER 1 $s'_n = s_n \ell / \pi c$
1	-.0084134±J1.5081822
2	-.00091777±J2.7579859
3	-.0038086±J3.7944657
4	-.0014096±J4.7144142
5	-.0025202±J5.5619009
6	-.0017633±J6.3647334
7	-.0021664±J7.1453109
8	-.0026354±J7.6904280
9	-.0029516±J8.5641276
10	-.0029193±J9.4361272
11	-.00282757±J9.70518
12	-.0037920±J10.3082632
13	-.0038233±J11.320626
14	-.0037931±J12.1376438

Table 1. First Layer Normalized Natural Frequencies of an 8-Turn Helix Over a Ground Plane

It has been suggested by some authors that a dipole is a good approximation for a helix. In figure 2 the trajectories of the natural frequencies are shown as the pitch angle α is changed. As can be seen the natural frequencies change quite drastically as the pitch angle is changed. Note that as the pitch angle is changed, while keeping the radius of the helix, number of turns and the wire radius constant, the imaginary part of the natural frequency drops. At the same time, the real part (damping) decreases. This implies that the antenna is becoming a better radiator. However, if the pitch angle is increased beyond a certain point, in the case of the first natural frequency beyond 45° , the damping constant starts to increase and becomes a constant equal to that of a straight thin wire of wire radius a and length ℓ . In figure 3 the trajectories of the natural frequencies are plotted by keeping the total length of the wire, radius of the wire and the radius of the helix constant, while changing the number of turns which in turn changes the pitch angle. This shows how the natural frequencies change as a straight wire becomes a helix, while preserving the total length.

If the aim is to design an optimum helical antenna, one can plot the trajectories of the natural frequencies of the helix by changing the pitch angle and by changing the radius of the helix and arrive at optimum figures for the radius of the helix and the pitch angle based on the damping constants. It is also interesting to note from the natural frequencies shown in table 1 that the helix is a poor radiator at low frequencies when the pitch angle is small. If the operating frequency is close to the loop resonance of the helix, it starts to become a better radiator.

Short circuit natural modes for the helix under consideration can be evaluated by solving the homogeneous equation

$$(\tilde{Z}_{n,m}) (\tilde{v}_m) = (\tilde{0}) \quad (4.8)$$

where $\tilde{Z}_{n,m}$ is the NXN impedance matrix evaluated at the natural frequency s_n . The natural mode \tilde{v}_n is calculated by converting

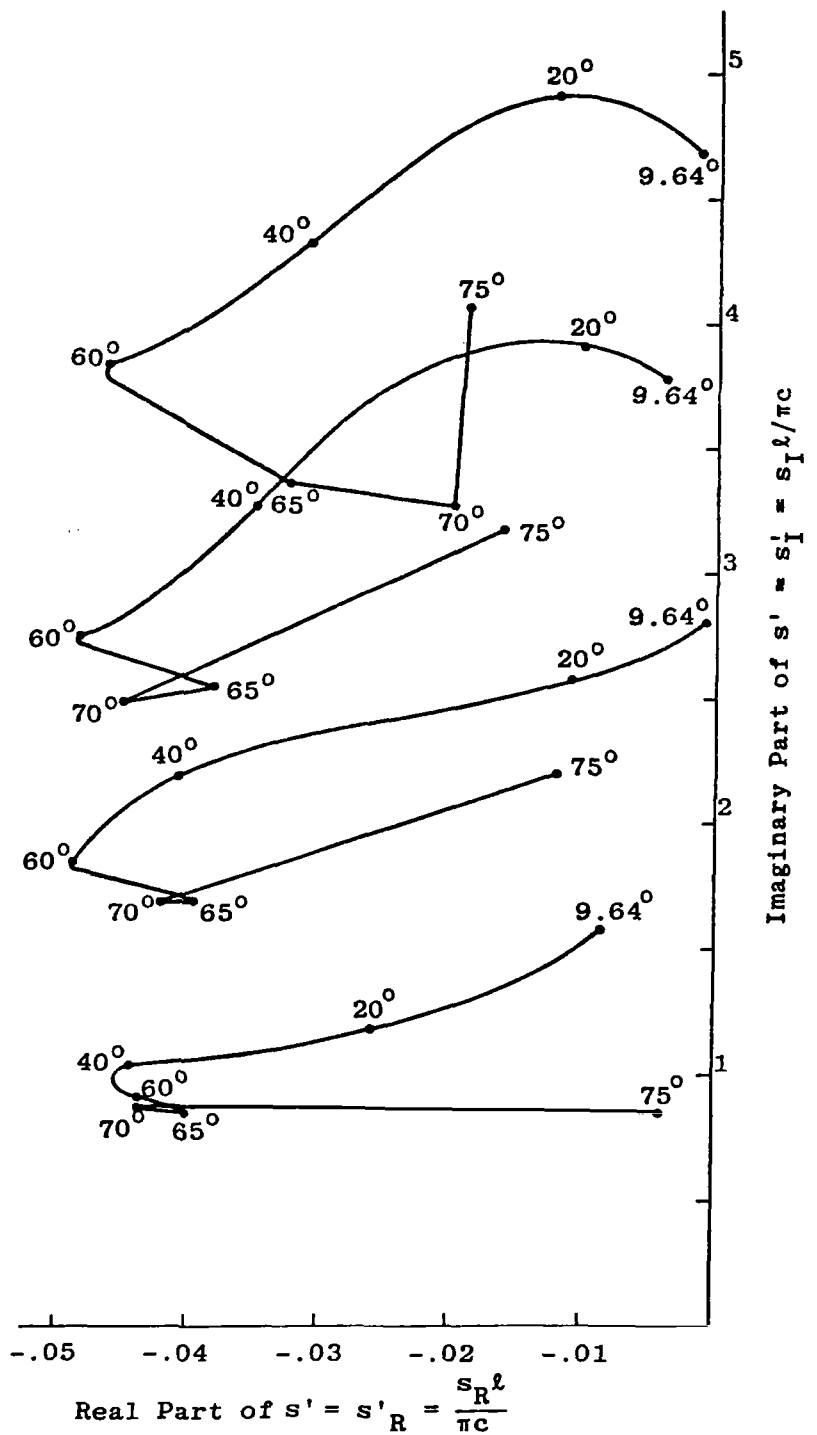


Figure 2. Movement of the Natural Frequencies as the Pitch Angle of the Helix is Changed. (Length of the Wire is not Kept Constant, Numbers Shown are Pitch Angles in Degrees. Sharp Corners are Due to Insufficient Number of Points).

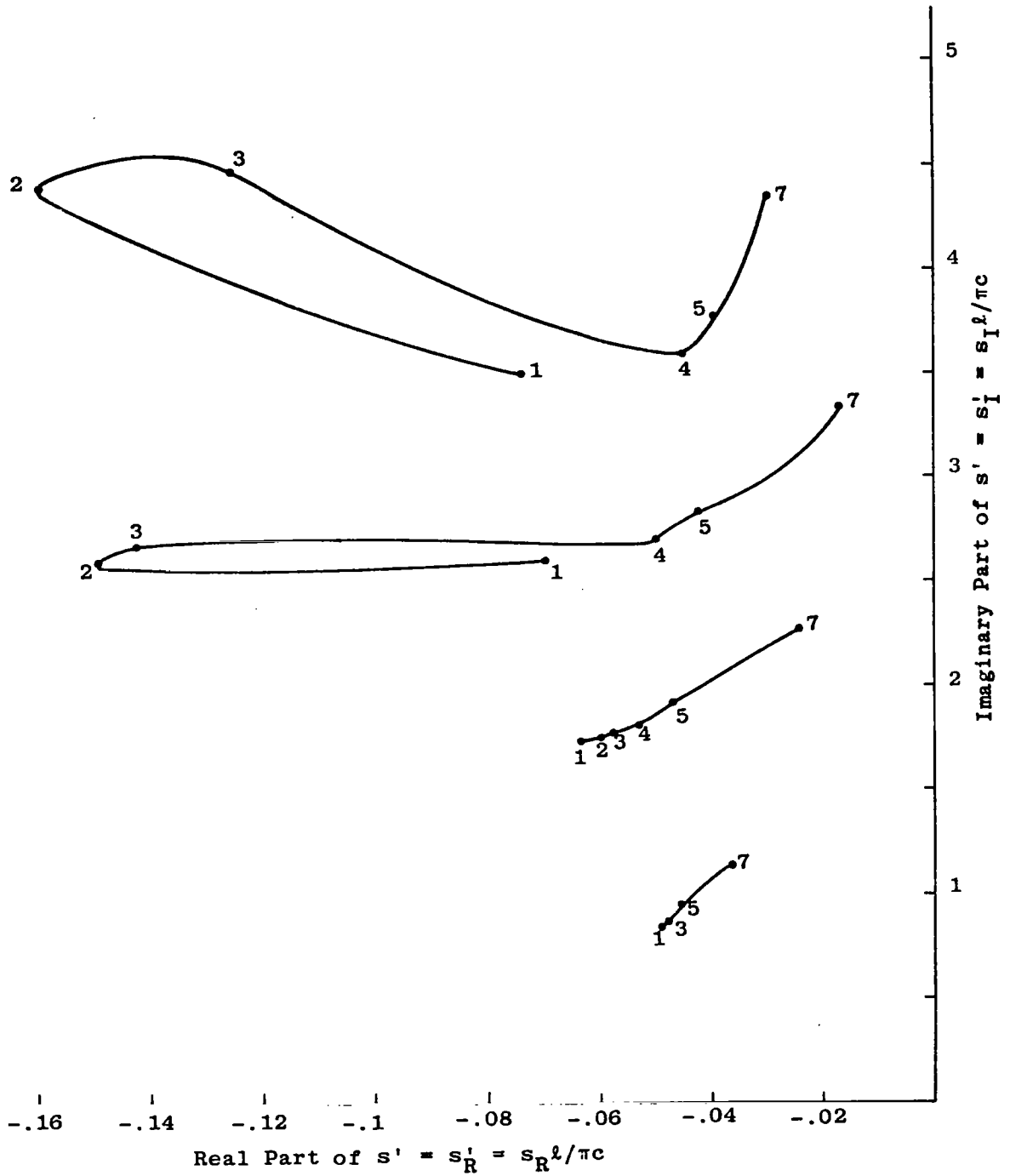


Figure 3. Movement of the Natural Frequencies as the Number of Turns of the Helix are Changed While Keeping the Total Length of the Wire Constant (Helix is Assumed to be Over a Ground Plane, Numbers Shown are the Number of Turns of the Helix).

equation 4.8 into a $N \times N - 1$ inhomogeneous set of equations which are solved using Householder's triangularization procedure.¹⁰ The natural modes have been normalized to have imaginary part to be zero at the peak value of the natural mode. In figure 4 the real part of the normalized natural modes are plotted for the first four natural frequencies. Imaginary parts of the natural frequencies are not shown because they are a strong function of the accuracy of the impedance matrix.¹¹ In addition, the peak of the imaginary part of the natural mode is approximately an order of magnitude below the peak of the real part. The natural modes shown in figure 4 are only for half the antenna. For the image part of the antenna, the natural mode can be obtained by taking the images for odd modes, while the even modes are obtained by taking the image with a sign reversal. Comparing the natural modes of the helix with those of a straight wire, the real parts are identical. This is the primary reason why the natural modes have not been calculated for higher order natural frequencies.

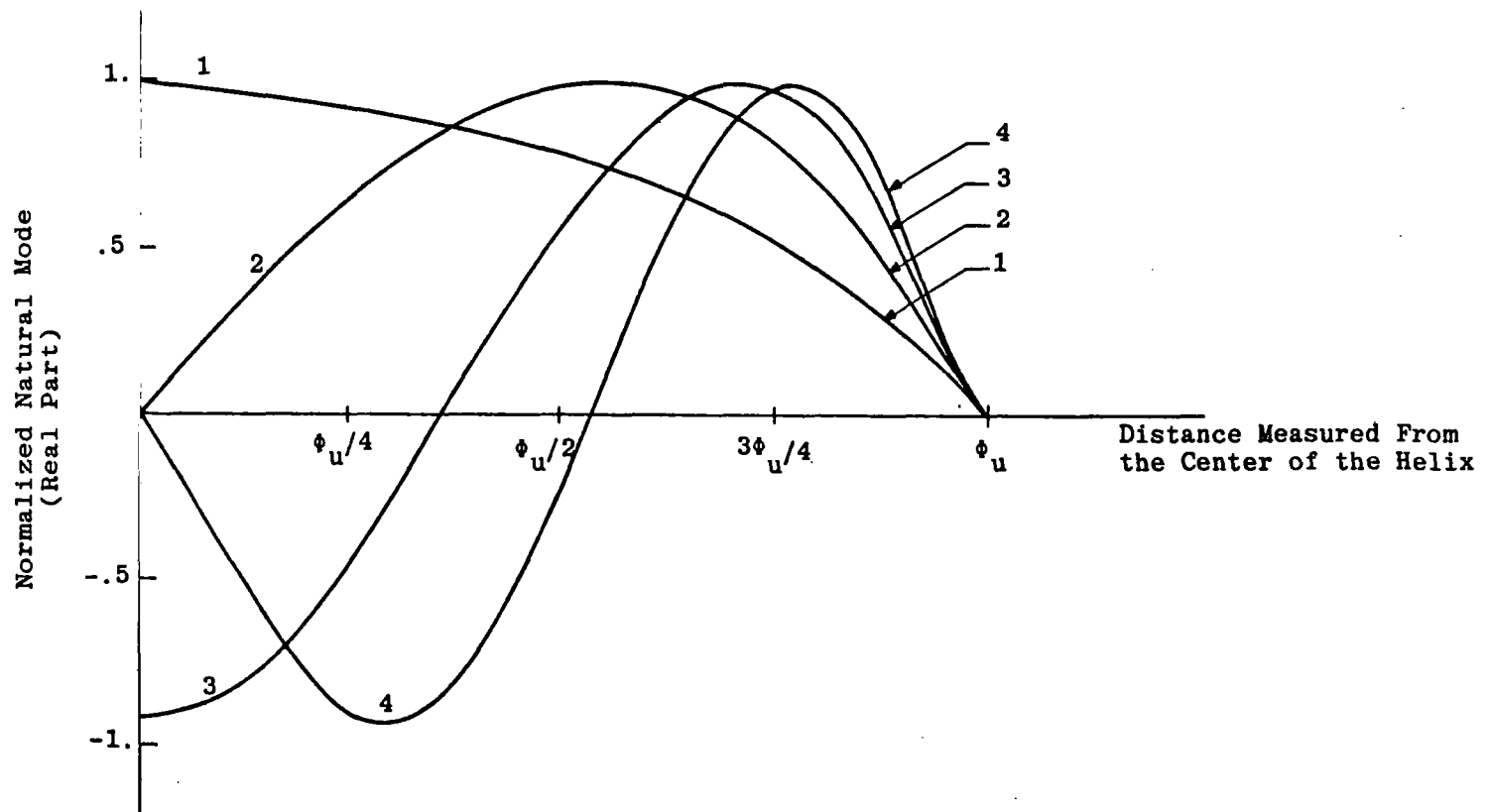


Figure 4. Normalized Real Parts of the Natural Modes for the First Layer, First Four Natural Frequencies.

V. Transient Response of a Helical Antenna

In this section we calculate the transient response of the helical antenna. The antenna is assumed to be on a perfectly conducting ground plane. The gap in the antenna is assumed to be a delta gap and it is further assumed that the antenna is terminated in load of $Z_L = 50\Omega$. If we let $\tilde{I}_{sc}(s)$ represent the short circuit current induced at the short circuited terminals of the antenna, $Y_a(s)$ the terminal admittance of the antenna and $Y_L(s)$ the load admittance, the equivalent circuit representation at the terminals of the antenna is as shown in figure 5.

Using the Singularity Expansion Method (SEM), the short circuit current induced due to an incident field \vec{E}_{inc} can be written as

$$\tilde{I}_{sc}(\xi, s) = -s\epsilon_0 \sum_n \left(\frac{1}{s-s_n} \right) \frac{\langle \tilde{I}_n(\xi) \vec{I}_\xi; \vec{E}_{inc}(\xi, s) \rangle}{B_n} \tilde{I}_n(\xi) \quad (5.1)$$

where the entire function contribution is ignored, s_n represents the n th short circuit natural frequency, \tilde{I}_n the corresponding short circuit natural mode and

$$B_n = \langle \tilde{I}_n(\xi) \vec{I}_\xi \cdot \vec{I}(\xi, \xi'); \tilde{I}(\xi') \vec{I}_\xi \rangle \quad (5.2)$$

which can be approximated as

$$B_n \approx - \frac{\Omega l s_n}{4\pi c^2} \quad (5.3)$$

For the purposes of numerical evaluation, the incident field is assumed to be a planewave, uniform over the length and circumference of the helix and is assumed to be along the axis of the helix. Under these assumptions, equation 5.1 can be rewritten as

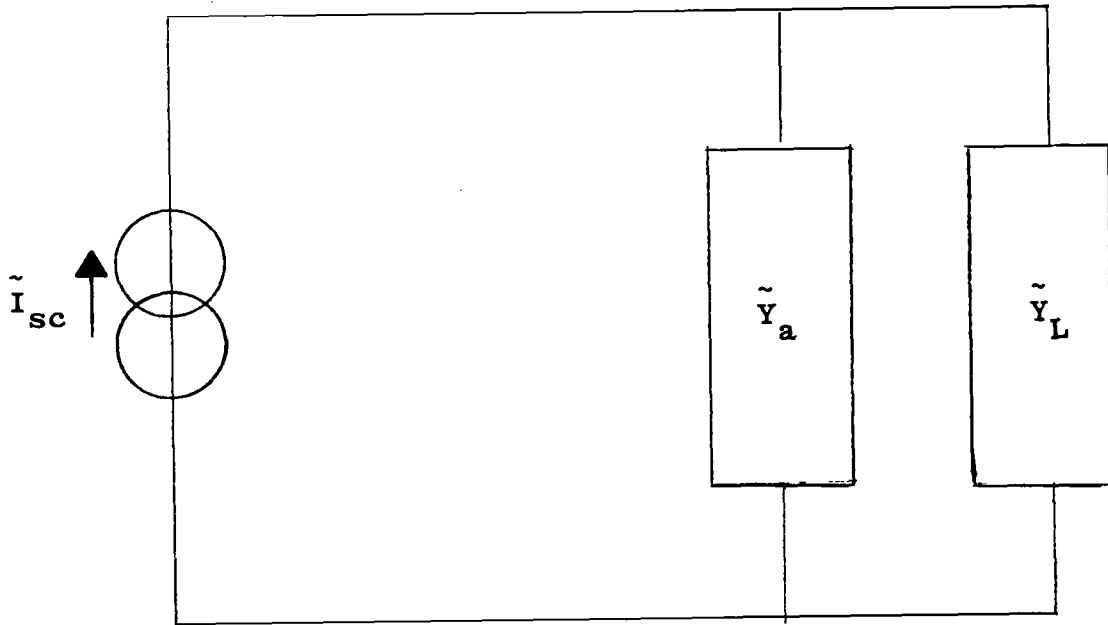


Figure 5. Equivalent Circuit at the Terminals of the Antenna.

$$\tilde{I}_{sc}(\xi, s) = \frac{4\pi c}{\Omega \ell Z_0} \sum_n \frac{s}{s_n(s-s_n)} \tilde{E}_{inc} \langle \tilde{I}_n(\xi) \hat{I}_\xi; \hat{I}_z \rangle \tilde{I}_n(\xi) \quad (5.4)$$

Using equation 5.1, the terminal admittance is calculated as discussed in reference 12. An equivalent circuit representation as shown in figure 5 was constructed with the short circuit current source, terminal admittance and the load admittance. Using these admittances, the terminal voltage can be written as

$$\tilde{V}(0, s) = \frac{4\pi c}{\Omega \ell Z_0} \left(\frac{1}{\tilde{Y}_L(s) + \tilde{Y}_a(s)} \right) \sum_{n \equiv \text{odd}} \frac{s}{s_n(s-s_n)} \tilde{E}_{inc} \langle \tilde{I}_n(\xi) \hat{I}_\xi; \hat{I}_z \rangle \tilde{I}_n(0) \quad (5.5)$$

Three special cases of the incident field are considered for numerical verification purposes. The first involves a rectangular pulse while the other two are triangular pulses incident on the helix. The incident pulses are assumed to have unit peak amplitude. In figures 6, 7 and 8 the incident waveform and the induced terminal voltages are shown. For comparison purposes, the measured waveform¹³ sample points are shown up to about 20 ns. Points beyond this time are not shown because of the lack of digitized waveforms.

Comparing the measured and calculated terminal voltages the general shapes of the waveforms are identical even for a fast pulse of total duration 1.5 ns. The zero crossings are within 10% of the measured values while the peaks agree to within 10% up to approximately 80 ns. Considering the approximations used, the results are very good. Differences in the measured and calculated responses can be attributed to the following points: (1) The measurements were made in a simulator which is quite small. As a consequence interaction between multiple images of the helix may be large. However, this fact was not used in the numerical evaluation. (2) The incident field has been assumed to be uniform over the helix. However, this is only true for wavelengths large compared to the length of the antenna. For fast

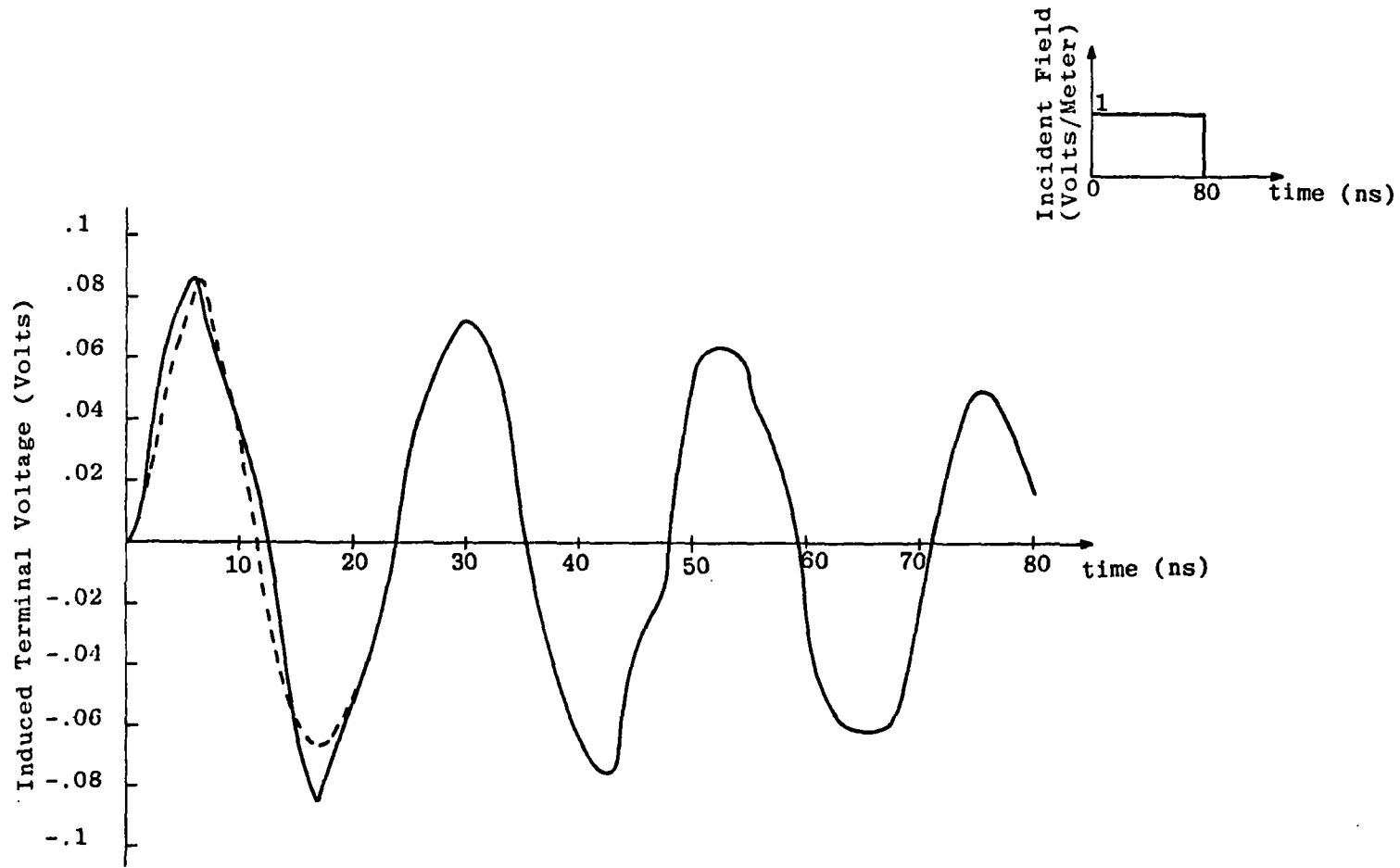


Figure 6. Response of a Helical Antenna to a Planewave Rectangular Incidence Pulse of 1V/m Peak Amplitude (Dots Represent Measured Data).

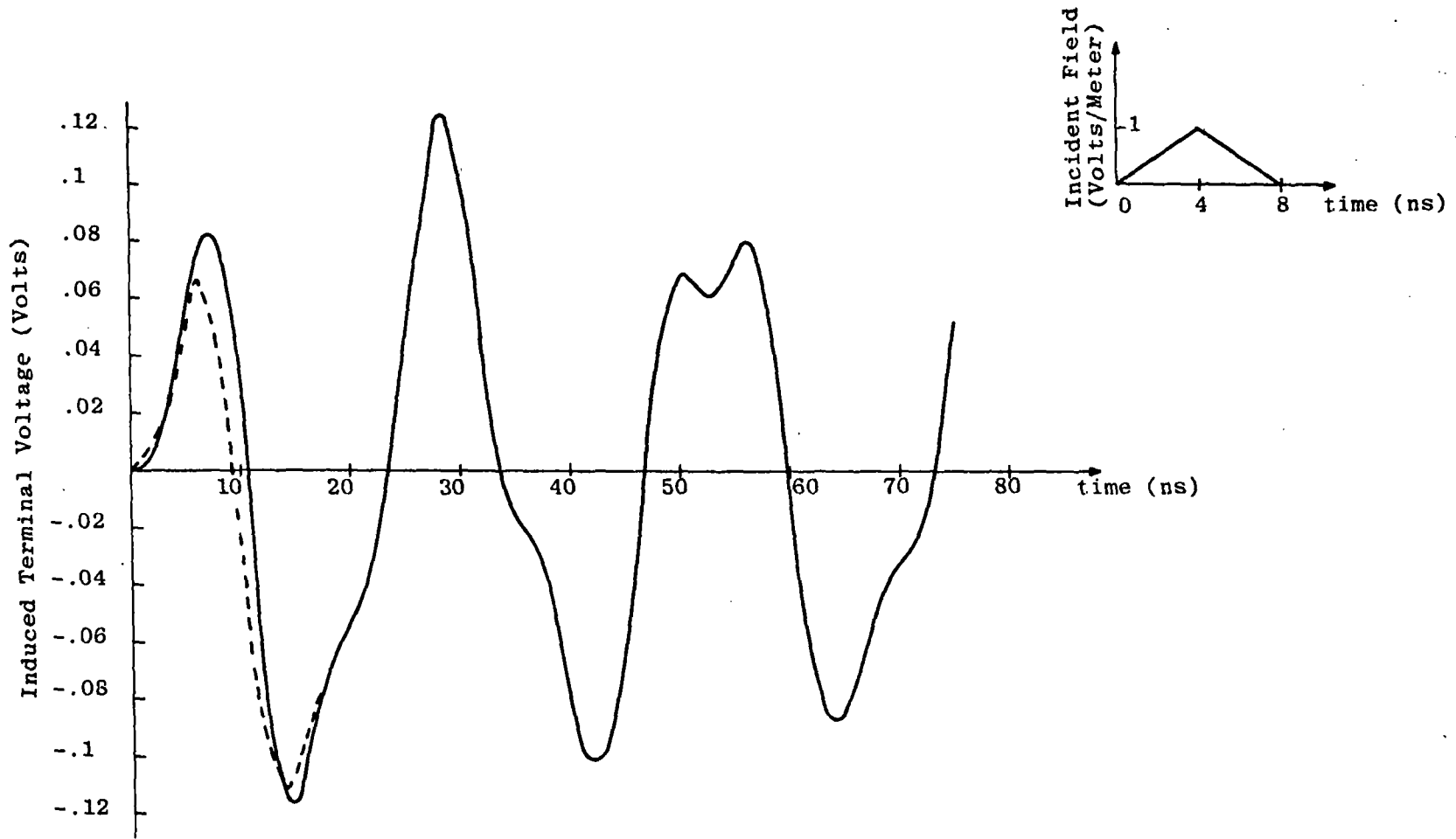


Figure 7. Response of a Helical Antenna to a Planewave Triangular Incidence Pulse of 1V/m Peak Amplitude (Dots Represent Measured Data).

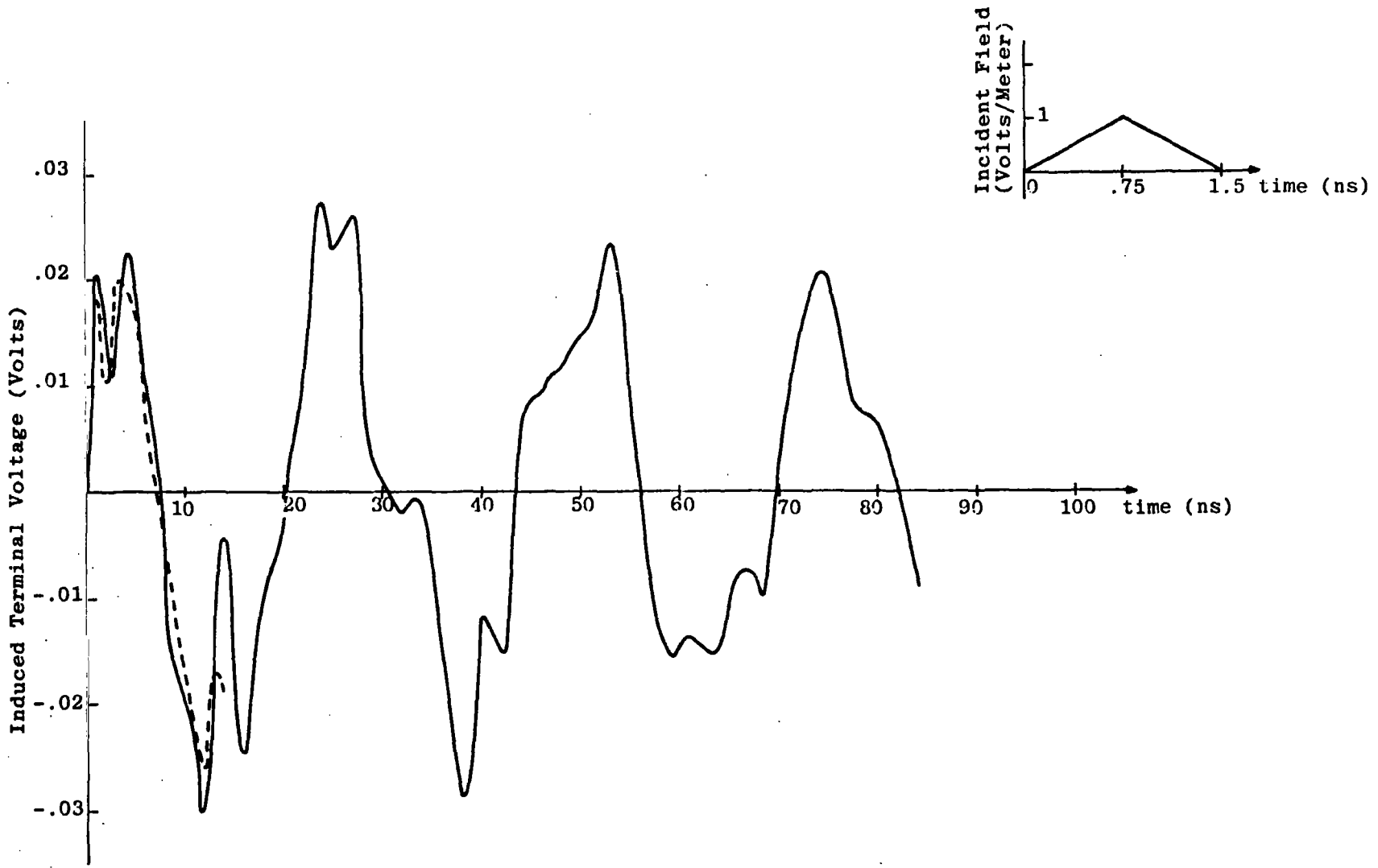


Figure 8. Response of a Helical Antenna to a Planewave Triangular Incidence Pulse of 1v/m Peak Amplitude (Dots Represent Measured Data).

rise time pulse as has been used in our numerical evaluation, this condition is not satisfied. Inclusion of the spatially varying field would have complicated the calculations and, in addition, does not seem to influence the terminal voltages to any large degree. (3) The incident field was assumed to be a **plane wave**. However, the simulator used was quite small and the incident field was probably nearer to a spherical wave than a **plane wave**. This would introduce errors in the analytical calculations.¹⁴ (4) For lack of a better description of the gap region, the gap was assumed to be a delta gap. This of course would change the low frequency input impedance which in turn would change the late time response of the antenna. Even with the approximations that have been made, the results are quite good and it is encouraging to see the measured and calculated values agree so well.


VI. Conclusions

In this report, two integral equations for a helical antenna were developed. Using the Hallén type integral equation, natural frequencies and natural modes of a loosely wound helix were calculated. An integral equation of the Pocklington type was developed for a helical antenna for numerical purposes. Using this equation, natural frequencies and natural modes of a given helix are calculated.

Using the Singularity Expansion Method (SEM), the short circuit current is calculated. Using this short circuit current, the load admittance and the terminal admittance, an expression for the terminal voltage was developed. The induced terminal voltage was calculated for three different incident pulses and comparisons were made with the measured values. The numerical results agree very well with the calculated results. The zero crossing and the peak values agree to within 10% of the measured results.

VII. References

1. C.E. Baum, "On the Singularity Expansion Method for the Solution of Electromagnetic Interaction Problems," Interaction Notes, Note 88, December 1976.
2. K.K. Mei, "On Integral Equations of Thin Wire Antennas," IEEE Trans. Antennas and Propagation, Vol. AP13, pp. 374-378, May 1965.
3. E. Hallén, "Über die Elektrischen Schwingungen in Drahtformigen Leitern," Uppsala Univ., Årsskrift, No. 1, pp. 1-102, 1930.
4. L. Marin, "Natural Modes of Certain Thin Wire Structures," Interaction Notes, Note 186, August 1974.
5. R.W.P. King, Theory of Linear Antennas, Harvard University Press, Cambridge, Mass., 1956.
6. I.S. Gradshteyn and I.W. Ryzhik, Table of Integrals Series and Products, Academic Press, New York, 1962.
7. G.A. Thiele, Computer Techniques in Electromagnetics, R. Mittra, editor, Pergamon Press, 1973.
8. R.F. Harrington, Field Computation by Moment Method, Macmillan, 1962.
9. B.K. Singaraju, D.V. Giri and C.E. Baum, "Further Developments in the Application of Contour Integration to the Evaluation of the Zeros of Analytic Functions and Relevant Computer Programs," Mathematics Notes, Note 42, March 1976.
10. A.S. Householder, "Unitary Triangularization of a Non Symmetric Matrix," J. of the Asso. for Comp. Mach., October 1958.
11. B.K. Singaraju, "Dependence of Natural Frequencies and Natural Modes on the Accuracy of the Impedance Matrix," Mathematics Note, to be published.
12. B.K. Singaraju and C.E. Baum, "Single Port Equivalent Circuits for Electric Dipole Antennas," Interaction Notes, *to be published*.

- 
13. "Response of GPS Helix to a Planewave." IRT Corporation.
 14. C.E. Baum, J.P. Castillo and J.K. Little, "Errors in Electromagnetic Coupling Coefficients Due to Wavefront Nonplanarity," Sensor and Simulation Notes, to be published.